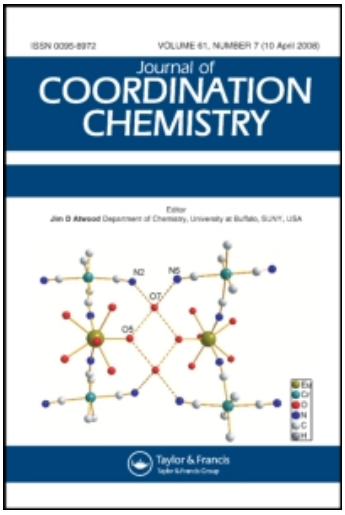

Journal of Coordination Chemistry
Publication details, including instructions for authors and subscription information:
http://www.informaworld.com/smpp/title~content=t713455674

Structural studies on platinum alkene complexes and precursors

Ruslan S. Pryadun[a]; Oksana O. Gerlits[a]; Jim D. Atwood[a]
[a] Department of Chemistry, University at Buffalo, The State University of New York, Buffalo, NY 14260-3000

To cite this Article Pryadun, Ruslan S. , Gerlits, Oksana O. and Atwood, Jim D.(2006) 'Structural studies on platinum alkene complexes and precursors', Journal of Coordination Chemistry, 59: 1, 85 — 100
To link to this Article: DOI: 10.1080/00958970500368267
URL: http://dx.doi.org/10.1080/00958970500368267

Journal of Coordination Chemistry
Vol. 59, No. 1, January 2006, 85–100

Taylor & Francis
Taylor & Francis Group

Structural studies on platinum alkene complexes and precursors

RUSLAN S. PRYADUN, OKSANA O. GERLITS and JIM D. ATWOOD*

Department of Chemistry, University at Buffalo,
The State University of New York, Buffalo, NY 14260-3000

(*Received in final form 20 September 2005*)

A number of platinum complexes, precursors to alkene complexes ($Pt_2Cl_4(PPh_3)_2$ and *cis*-$PtCl_2(CH_3CN)(PPh_3)$), alkene complexes (*cis*-$PtCl_2(C_2H_4)(PPh_3)$, *cis*-$PtCl_2(C_3H_6)(PPh_3)$ and *cis*-$PtCl_2(1\text{-}C_6H_{12})(PPh_3)$), the diamination product of a 1,3-butadiene platinum complex and the 1,2,3,4-tetramethylcyclobutadiene complex resulting from dimerization of 2-butyne have been synthesized, characterized and the structures determined by X-ray diffraction. The ethylene complex, *cis*-$PtCl_2(C_2H_4)(PPh_3)$, has been a useful reagent for preparing other alkene complexes. Reaction of a bound butadiene complex with diethylamine yielded a diamination product with anti-Markovnikov stereochemistry. An attempt at binding *cis*-butyne to the metal center resulted in metal-assisted formation of 1,2,3,4-tetramethylcyclobutadiene with previously unreported geometry.

Keywords: Platinum; Alkenes; Cyclobutadienes; Butadiene; Hydroamination

1. Introduction

Since the discovery of Zeise's salt in 1827 [1], platinum alkene complexes have occupied a central position in coordination chemistry. Pt(II) complexes with, effectively, only one geometry and good stability provide excellent models for a wide variety of bonding, structural and reactivity studies.

In the course of our studies of nucleophilic attack on alkenes coordinated to platinum [2], we have prepared and structurally characterized two platinum complexes as potential precursors to alkene complexes, three alkene complexes and one product of amine attack on coordinated 1,3-butadiene. Compounds **1**, $Pt_2Cl_4(PPh_3)_2$ and **2**, *cis*-$PtCl_2(CH_3CN)(PPh_3)_2$ readily provide an open site for ligand addition. Compounds **3**, *cis*-$PtCl_2(C_2H_4)(PPh_3)$, **4**, *cis*-$PtCl_2(C_3H_6)(PPh_3)$ and **5**, *cis*-$PtCl_2(1\text{-}C_6H_{12})(PPh_3)$ contain coordinated ethylene, propene and 1-hexene. Compound **6**, $(PPh_3)ClPt(\mu - NEt_2CH_2CHCHCH_2NEt_2)PtCl(PPh_3)$ results from the diamination

*Corresponding author. Email: jatwood@buffalo.edu

Journal of Coordination Chemistry
ISSN 0095-8972 print: ISSN 1029-0389 online © 2006 Taylor & Francis
DOI: 10.1080/00958970500368267

of coordinated 1,3-butadiene. Compound **7**, $PtCl_2(\eta^4$-1,2,3,4-tetramethylcyclobutadiene)(PPh_3) results from dimerization of 2-butyne on the platinum center. The structures of **4** and **5** were previously reported as supplementary data, but not discussed [2]. The remainder are, to our knowledge, compounds for which structures have not been reported. The very similar structures allow direct comparisons.

2. Experimental

2.1. *Materials*

The following chemicals were used in the syntheses: K_2PtCl_4 and $H_2PtCl_6 \cdot H_2O$ were purchased from Strem Chemicals; PPh_3 was purchased from Aldrich Chemical Company and recrystallized from ethanol. $PtCl_2$ [3] and $PtCl_2(PPh_3)_2$ [4] were synthesized by literature procedures. Several deuterated solvents were utilized: dimethylformamide (C_3D_7ON), benzene (C_6D_6), methylene chloride (CD_2Cl_2) and chloroform ($CDCl_3$). All were purchased from Aldrich Chemical Company. Triply-distilled H_2O was kindly available from Dr. G. Nancollas's lab. Compressed air, Ar and N_2 were purchased from Praxair. Ethylene and propylene were purchased from Matheson. *cis*-2-Butene, 1-butene, and 2-butyne were purchased from Aldrich Chemical Company. All solvents were purchased from Aldrich Chemical Company and used as received without further purification unless otherwise stated.

2.2. *Instrumentation*

^1H, ^{31}P, ^{195}Pt spectra were recorded using a Varian VXR 400 MHz NMR spectrometer unless otherwise stated. ^{31}P NMR spectra were ^1H decoupled and referenced to an external sample of 85% H_3PO_4 in D_2O (reference was set to 0.00 ppm). ^{195}Pt NMR spectra were referenced to an external sample of 0.2 M K_2PtCl_4 (in 0.4 M KCl/D_2O), in which the reference was set to −1627.00 ppm [5]. All ^1H spectra were referenced to TMS (reference set to 0.00 ppm). All 2-D and ^{13}C spectra were recorded on the Varian VXR 500 MHz NMR spectrometer. ^{13}C spectra were ^1H decoupled and referenced to TMS (set to 0.00 ppm). Aromatic protons in the region of 7–8 ppm were excluded from discussion for simplicity purposes. All chemical shifts are reported in parts per million (ppm) and all coupling constants (J) are in Hz. Whenever possible ^1H and ^{31}P spectra were integrated and relative abundance for each species present in a given sample was assigned.

All gas chromatographic analyses were performed using a Hewlett Packard 5890 series gas chromatograph with a flame ionization detector and an Altech AT-WAX capillary column: 30 m (length) × 0.25 mm (internal diameter) × 0.20 μm (film thickness). All qualitative analyses were done by comparing product chromatograms with those of authentic samples.

X-ray diffraction data were collected at 90 K using a Bruker SMART1000 CCD diffractometer [6] installed at a rotating anode source (Mo Kα radiation, $\lambda = 0.71073$ Å), and equipped with an Oxford Cryosystems nitrogen flow apparatus. For **1** and **4** the collection method involved 0.3° scans in ω at 28° in 2θ. Data integration was carried out using SAINT V6.02 [6] with reflection spot size optimization. Absorption corrections were made with the program SADABS [7]. The structure was

solved by the direct methods procedure and refined by least-squares methods based on F^2 using SHELXS-97 and SHELXL-97 [8]. For complexes **2**, **3**, **5**, **6** and **7** the data were collected by the rotation method with 0.3° frame-width (ω scan) and 10 s (for **2** and **3**) and 20 s (for **5**, **6** and **7**) exposure per frame. Four sets of data (600 frames in each set) were collected, nominally covering half of the reciprocal space. The data were integrated, scaled, sorted and averaged using the SMART software package [9]. The structures were solved by the Patterson method using SHELXTL NT Version 5.10 [10]. The structures were refined by full-matrix least squares against F^2. Non-hydrogen atoms were refined anisotropically and hydrogen atoms were geometrically fixed and allowed to ride on the respective atoms (table 1).

2.3. *Syntheses*

All syntheses were performed via standard Schlenk techniques utilizing a double-manifold vacuum system with Ar gas flow. All of the solvents were degassed prior to use.

***trans*-$Pt_2Cl_4(PPh_3)_2$, 1 [11].** The following method was adapted from a previously published procedure. A 100 mL round bottom flask was charged with 0.292 g (1.1 mmol) of $PtCl_2$ and 0.711 g (0.9 mmol) of $PtCl_2(PPh_3)_2$. Both reactants were dissolved in 25 mL of 1,1,2,2-tetrachloroethane and a reflux condenser with N_2 output was attached to the round bottom flask. The solution was refluxed for 60 min, after which it was filtered while hot through a fine frit. Precipitation of the product was achieved by addition of 65 mL of hexanes to the filtrate. The bright orange product was collected using a fine frit, dried under vacuum and weighed. The yield of the crude product was 0.951 g, 36.8%, based on the starting $PtCl_2(PPh_3)_2$. The product was recrystallized from CH_2Cl_2. $^{31}P\{^1H\}$ NMR ($CDCl_3$; δ(ppm)): 4.71 (s, $J_{(Pt-P)} = 4100$ Hz).

$PtCl_2(C_2H_4)(PPh_3)$, 3. A suspension of dichloroplatinum(II) (1 g, 3.759 mmol) and triphenylphosphine (0.986 g, 3.759 mmol) in 20 mL DMF was stirred in a Paar apparatus under 300 psi of ethylene for 48 h. The resulting yellow solution was treated with 80 mL of diethyl ether, causing precipitation of the white crystalline solid. The latter was washed with diethyl ether and several 20 mL portions of pentane. The product was obtained in 87% yield, based on starting dichloroplatinum(II), as a white powder. $^{31}P\{^1H\}$ NMR ($CDCl_3$; δ(ppm)): 14.6 (s, $^1J_{P-Pt} = 3295$). ^1H NMR ($CDCl_3$; δ(ppm)): 4.1 (br, 4H). ^{195}Pt NMR ($CDCl_3$; δ(ppm)): 4047.5 (d, $^1J_{P-Pt} = 3295$).

$PtCl_2$(alkene)(PPh_3) [12]. Other alkene complexes can be synthesized through the replacement of ethylene with the higher olefin. A glass vessel inside a Paar apparatus was charged with 0.793 mmol of *cis*-$PtCl_2(PPh_3)(C_2H_4)$ in 15 mL of chloroform. The glass vessel was pressurized to 5 atm of propene and shaken for 48 h. The resulting solution contained a suspension of white solid. Toluene was added and chloroform was removed *in vacuo*. A white solid was obtained by filtration and washed several times with toluene. The yield of *cis*-$PtCl_2(PPh_3)(C_3H_6)$ is a function of time, if the pressure is held constant, with the reversible reaction taking five days to maximize product.

$PtCl_2(C_3H_6)(PPh_3)$, 4. ^{31}P NMR ($CDCl_3$; δ(ppm)): 10.96 (s, $^1J_{(P-Pt)} = 3305$). ^{195}Pt NMR ($CDCl_3$; δ(ppm)): 3984.04 (d, $^1J_{P-Pt} = 3305$). ^1H NMR ($CDCl_3$;

Table 1. Crystal data and structure refinement for compounds **1**–**7**.

Compound	**1**	**2**	**3**	**4**	**5**	**6**	**7**
Empirical formula	$C_{20}H_{17}Cl_2PPt$	$C_{20}H_{18}Cl_2NPPt$	$C_{20}H_{19}Cl_2PPt$	$C_{21}H_{21}Cl_2PPt$	$C_{24}H_{27}Cl_2PPt$	$C_{52}H_{60}Cl_2N_2P_2Pt_2$	$C_{26}H_{27}Cl_2PPt$
Crystal shape	Plate	Plate	Parallelepiped	Prism	Prism	Plate	Parallelepiped
Crystal system, space group	Monoclinic, $P2_1/c$	Triclinic, $P\bar{1}$	Tetragonal, $P4_1$	Monoclinic, $P2_1/n$	Triclinic, $P\bar{1}$	Triclinic, $P\bar{1}$	Orthorhombic, $P2_12_12_1$
Unit cell dimensions							
a (Å)	10.3355(11)	8.9295(3)	7.9351(2)	11.106(1)	8.8157(4)	10.2935(5)	8.3223(3)
b (Å)	17.7892(18)	10.6561(4)	7.9351(2)	14.117(1)	9.5186(4)	10.3771(5)	16.5519(5)
c (Å)	12.4170(12)	11.4834(4)	30.3082(10)	13.274(1)	14.6356(6)	14.2094(7)	17.5260(5)
α (°)	90	117.317(1)	90	90	90.426(1)	77.626(1)	90
β (°)	99.776(3)	98.111(1)	90	98.934(3)	106.265(1)	69.943(1)	90
γ (°)	90	95.459(1)	90	90	102.784(1)	86.512(1)	90
Volume (Å^3)	2249.8(4)	945.11(6)	1908.38(9)	2055.7(3)	1146.58(9)	1392.5(1)	2414.2(1)
Z, Calculated density (g cm^{-3})	4, 2.055	2, 2.001	4, 1.936	4, 1.843	2, 1.774	1, 1.812	4, 1.751
Absorption coefficient (mm^{-1})	7.026	7.793	7.715	7.165	6.429	5.592	6.111
Max 2θ (°)	56.58	56.58	68.74	56.84	61.12	66.06	65.48
Reflections collected/unique	18616/5555 [$R_{int} = 0.0325$]	11108/4630 [$R_{int} = 0.0246$]	39821/7637 [$R_{int} = 0.025$]	17438/5151 [$R_{int} = 0.0383$]	26959/7023 [$R_{int} = 0.0450$]	29240/10381 [$R_{int} = 0.0313$]	34234/8101 [$R_{int} = 0.024$]
Goodness-of-fit on F^2	1.033	1.040	0.849	1.031	1.039	1.239	0.819
Final R indices [$I > 2\sigma(I)$]	$R_1 = 0.0471$, $wR_2 = 0.1113$	$R_1 = 0.0164$, $wR_2 = 0.0414$	$R_1 = 0.0133$, $wR_2 = 0.0290$	$R_1 = 0.0220$, $wR_2 = 0.0529$	$R_1 = 0.0307$, $wR_2 = 0.0729$	$R_1 = 0.048$, $wR_2 = 0.1537$	$R_1 = 0.014$, $wR_2 = 0.030$

δ (ppm)): Varian 500 MHz 1.92 (br, 3H, CH_2CHCH_3), 3.54 (br, H, CH_2CHCH_3), 4.35 (br, 2H, CH_2CHCH_3).

$PtCl_2$(1-hexene)(PPh_3), 5. $^{31}P\{^1H\}$ NMR ($CDCl_3$; δ (ppm)): 11.27 (s, $^1J_{P-Pt} = 3318$). ^{195}Pt NMR ($CDCl_3$; δ (ppm)): 3999.31 (d, $^1J_{P-Pt} = 3227$). ^1H NMR (excluding aromatic protons) ($CDCl_3$; δ (ppm)): 0.87 (t, $J_{(H-H)} = 7.51$, 3H, $CH_2CHCH_2CH_2CH_2CH_3$), 1.27 (br, 2H, $CH_2CHCH_2CH_2CH_2CH_3$), 1.42 (br, H, $CH_2CHCH_2CHHCH_2CH_3$), 1.71 (br, H, $CH_2CHCH_2CHHCH_2CH_3$), 1.85 (br, H, $CH_2CHCHHCH_2CH_2CH_3$), 2.55 (br, H, $CH_2CHCHHCH_2CH_2CH_3$), 3.52 (br, H, $CH_2CHCH_2CH_2CH_2CH_3$), 4.19 (br, H, $CHHCHCH_2CH_2CH_2CH_3$), 4.36 (br, H, $CHHCHCH_2CH_2CH_2CH_3$).

$PtCl_2$(1,3-butadiene)(PPh_3). $^{31}P\{^1H\}$ NMR ($CDCl_3$; δ (ppm)): 10.52 (s, $^1J_{P-Pt} = 3223$). ^{195}Pt NMR ($CDCl_3$; δ (ppm)): 3223.29 (d, $^1J_{P-Pt} = 3311$). ^1H NMR ($CDCl_3$; δ (ppm)): 3.41 (m, $J_{(H-H)} = 4.40$, 2H), 4.52 (m, $J_{(H-H)} = 13.20$, 2H), 5.56 (br, 2H).

***cis*-$PtCl_2$(2-butyne)(PPh_3) and $PtCl_2(\eta^4$-$C_4Me_4)(PPh_3)$, 7.** A procedure similar to that for **4** utilizing 2-butyne resulted in a mixture containing *cis*-$PtCl_2$(2-butyne)(PPh_3) and $PtCl_2$(1,2,3,4-tetramethylcyclobutadiene)(PPh_3).

***cis*-$PtCl_2$(2-butyne)(PPh_3).** $^{31}P\{^1H\}$ NMR ($CDCl_3$; δ (ppm)): 11.79 (s, $^1J_{P-Pt} = 3675$). ^1H NMR ($CDCl_3$; δ (ppm)): 1.59 (br). ^{195}Pt NMR ($CDCl_3$; δ (ppm)): 3523 (d, $^1J_{P-Pt} = 3675$).

$PtCl_2(\eta^4$-$C_4Me_4)(PPh_3)$. $^{31}P\{^1H\}$ NMR ($CDCl_3$; δ (ppm)): 12.31 (s, $^1J_{P-Pt} = 4181$). ^1H NMR ($CDCl_3$; δ (ppm)): 1.39 (d, $^4J_{(H-P)} = 4.00$; $^3J_{Pt-H} = 20.74$ Hz). ^{195}Pt NMR ($CDCl_3$; δ (ppm)): 3332 (d, $^1J_{P-Pt} = 4181$).

2.4. *Methods for growing crystals*

***trans*-$Pt_2Cl_4(PPh_3)_2$.** Crystals of the platinum dimer were grown from *cis*-$PtCl_2(C_2H_4)(PPh_3)$ by diffusion of pentane into 1,1,2,2-tetrachloroethane. A supersaturated solution of *cis*-$PtCl_2(C_2H_4)(PPh_3)$ in 1,1,2,2-tetrachloroethane (2 mL) was placed into an arm of an H-tube. Into a different arm 10 mL of pentanes was added and both arms were capped. After 6 h light orange crystalline needles started to form. Crystals were isolated after decanting solvents and letting crystals dry inside the container.

***cis*-$PtCl_2(C_3H_6)(PPh_3)$, 4.** A solution of 1.1 M *cis*-$PtCl_2(C_2H_4)(PPh_3)$ in chloroform was placed under propylene (300 psi) for an extended period of at least 7 days. After depressurizing the autoclave small crystals were observed on the stirrer. Perforated surface of the container holding the solution possibly enhances crystal growth. Crystals appear to be of a light brown/beige color.

***cis*-$PtCl_2(C_6H_{12})(PPh_3)$, 5.** One arm of a two-armed H-tube was charged with 5 mL of 1.59 M solution of *cis*-$PtCl_2(C_6H_{12})(PPh_3)$ in 1,1,2,2-tetrachloroethane and 1 mL of 1-hexene. Into a second arm 15 mL of pentanes was added and both arms were capped with stoppers. Small yellow and orange crystals formed after 24 h. Orange crystals were identified as *trans*-$Pt_2Cl_4(PPh_3)_2$ by ^{31}P NMR. Slightly yellowish crystals were characterized by X-ray crystallography.

***cis*-$PtCl_2(PPh_3)(NCCH_3)$, 2.** Failed attempt at growing crystals of $PtCl_2(C_2H_4)(PPh_3)$ resulted in formation of $PtCl_2(NCCH_3)(PPh_3)$. The same procedure as for

cis-$PtCl_2(C_6H_{12})(PPh_3)$ was used except that acetonitrile was utilized as a solvent to dissolve *cis*-$PtCl_2(C_2H_4)(PPh_3)$. Crystals exhibited a slightly green appearance with a very well defined morphology.

$Pt_2Cl_2(PPh_3)_2[C_4H_6(NEt_2)_2]$, 6. Crystals of $Pt_2Cl_2(PPh_3)_2[C_4H_6(NEt_2)_2]$ were grown from a powder, containing a mixture of products formed after the reaction of platinum bound 1,3-butadiene and diethylamine, by diffusion. Several mL of a 0.84 M solution of the product in 1,1,2,2-tetrachloroethane was placed into one arm of an H-tube. The second arm was charged with 15 mL pentanes and both arms were capped. Pentane was allowed to diffuse into 1,1,2,2-tetrachloroethane for a period of 48 h at which point crystal growth was evident on the sides of the flask. Yellow crystals were isolated and washed with pentane.

$PtCl_2(\eta^4\text{-}C_4Me_4)(PPh_3)$, 7. A 1.5 M mixture of $PtCl_2(\eta^4\text{-}C_4Me_4)(PPh_3)$ and *cis*-$PtCl_2$(2-butyne)(PPh_3) in 1,1,2,2-tetrachloroethane was added to one arm of an H tube (10 mL). The second arm was charged with 20 mL of pentane and the H tube was capped with Teflon stoppers and left in the dark at room temperature for a period of nine days. Needle-like crystals appeared on the sides of the H tube with morphology and color like those of *trans*-$Pt_2Cl_4(PPh_3)_2$. Solvent was decanted and crystals were carefully removed from the vessel and washed with copious amounts of pentane and dried *in vacuo*.

3. Results and discussion

Alkene complexes. The bond distances and angles for complexes **3**–**5** (tables 2–4, respectively) show a square-planar platinum with the alkene perpendicular to the plane, as expected. The labeling diagrams are given in figures 1–3.

Comparison of the geometries for complexes **3**, **4** and **5** shows that the $Pt–C_{alkene}$ distance measured to the double bond centroid is shorter for C_2H_4 (2.034(2) Å) than C_3H_6 (2.052(3) Å) which is shorter than for 1-C_6H_{12} (2.058(5) Å). These distances are consistent with the observed reactivity trend where 1-hexene is more easily displaced than propene or ethene. The average $Pt–C_{alkene}$ bond distance is controlled by the asymmetry in binding of propene and 1-hexene to Pt. This asymmetry in platinum–carbon bond lengths, well known [13], is nicely illustrated in complexes **3**–**5**. For complex **3** the $Pt–C_{alkene}$ bond lengths are equivalent at 2.147(2) Å. For propene, in **4** the $Pt–C_{terminal}$ bond length is 2.146(3) Å while the $Pt–C_{internal}$ bond is 2.188(3) Å. The asymmetry is more pronounced for complex **5**, $Pt–C_{terminal} = 2.144(5)$ Å and $Pt–C_{internal} = 2.204(5)$ Å. Potential electronic rationales for the asymmetry [13] find no evidence in other aspects of the structures of **3**, **4** and **5**. The Pt–Cl bond *trans* to the alkene is shortest for complex **3** and almost equivalent for **4** and **5**. Predictions of preferred nucleophilic attack at the internal carbon for the electronic rationale are also counter to observations for reaction with $NHEt_2$ which shows a kinetic preference for the terminal carbon [2]. The structures of **3**, **4** and **5** show little evidence of steric factors causing the asymmetry of the alkene; angles around the Pt or P are not significantly changed from **3** to **5**. The *cis*-Pt–Cl bond is shortest for complex **5**.

The C–C bond of the alkenes, 1.387(4), 1.394(5) and 1.405(8) Å for complexes **3**, **4** and **5**, respectively, show lengthening as the carbon chain is longer. Such lengthening is usually attributed to enhanced π-donation from the metal into the anti-bonding

Table 2. Bond lengths (Å) and angles (°) for $PtCl_2(C_2H_4)(PPh_3)$, **3**.

Pt(1)–C(1)	2.147(2)
Pt(1)–C(2)	2.147(2)
Pt(1)–P(1)	2.2536(5)
Pt(1)–Cl(1)	2.2964(5)
Pt(1)–Cl(2)	2.3436(6)
C(1)–C(2)	1.387(4)
C(1)–Pt(1)–C(2)	37.7(1)
C(1)–Pt(1)–P(1)	95.17(7)
C(2)–Pt(1)–P(1)	94.63(7)
C(1)–Pt(1)–Cl(1)	161.75(7)
C(2)–Pt(1)–Cl(1)	159.87(7)
Pt(1)–Pt(1)–Cl(1)	88.49(2)
C(1)–Pt(1)–Cl(2)	87.04(7)
C(2)–Pt(1)–Cl(2)	87.68(7)
P(1)–Pt(1)–Cl(2)	177.61(2)
Cl(1)–Pt(1)–Cl(2)	89.13(2)
C(2)–C(1)–Pt(1)	71.1(1)
C(1)–C(2)–Pt(1)	71.16(14)

Table 3. Bond lengths (Å) and angles (°) for $PtCl_2(C_3H_6)(PPh_3)$, **4**.

Pt(1)–C(1)	2.146(3)
Pt(1)–C(2)	2.188(3)
Pt(1)–P(1)	2.2610(7)
Pt(1)–Cl(1)	2.3195(8)
Pt(1)–Cl(2)	2.3623(8)
C(1)–C(2)	1.394(5)
C(2)–C(3)	1.497(6)
C(1)–Pt(1)–C(2)	37.52(14)
C(1)–Pt(1)–P(1)	95.58(10)
C(2)–Pt(1)–P(1)	91.06(10)
C(1)–Pt(1)–Cl(1)	164.29(11)
C(2)–Pt(1)–Cl(1)	158.11(11)
P(1)–Pt(1)–Cl(1)	87.35(3)
C(1)–Pt(1)–Cl(2)	88.13(10)
C(2)–Pt(1)–Cl(2)	93.87(10)
P(1)–Pt(1)–Cl(2)	175.05(3)
Cl(1)–Pt(1)–Cl(2)	88.21(3)
C(2)–C(1)–Pt(1)	72.9(2)
C(1)–C(2)–C(3)	127.1(4)
C(1)–C(2)–Pt(1)	69.6(2)
C(3)–C(2)–Pt(1)	113.2(3)

orbital of the alkene. Several studies indicate that π-donation from the alkene to the metal and back donation from the metal to the alkene destabilize the C–C bond [14]. Thus, the C–C bond distance for such analogous complexes indicate stronger bonding of the alkene to the platinum in the order, Pt–1-hexene > Pt–propene > Pt–ethylene [14]. This is contrary to the observed reactivity toward alkene loss and to the average $Pt–C_{alkene}$ bond distances which vary for $Pt–C_{centroid}$, $Pt–C_2H_4$, 2.034(2) Å; $Pt–C_3H_6$, 2.052(3) Å; $Pt–C_6H_{12}$, 2.058(5) Å. Calculations on a set of platinum complexes with strained olefins showed a clear trend of decreasing Pt–C bond lengths as C–C bond lengths increased [15]. The counterintuitive trend observed for $PtCl_2(alkene)(PPh_3)$ with longer $Pt–C_{(alkene)}$ bonds accompanied by longer C–C(alkene) bond lengths appears to have not been previously noticed and likely arises from a significant change in hydridization or "pyramidalization" [16].

Table 4. Bond lengths (Å) and angles (°) for *cis*-$PtCl_2(C_6H_{12})(PPh_3)$, **5**.

Pt(1)–C(1)	2.144(5)
Pt(1)–C(2)	2.204(5)
Pt(1)–P(1)	2.2517(8)
Pt(1)–Cl(1)	2.3149(9)
Pt(1)–Cl(2)	2.3514(9)
C(1)–C(2)	1.405(8)
C(2)–C(3B)	1.442(3)
C(2)–C(3A)	1.454(3)
C(1)–Pt(1)–C(2)	37.7(2)
C(1)–Pt(1)–P(1)	98.0(2)
C(2)–Pt(1)–P(1)	92.3(1)
C(1)–Pt(1)–Cl(1)	164.6(2)
C(2)–Pt(1)–Cl(1)	157.7(2)
P(1)–Pt(1)–Cl(1)	84.77(3)
C(1)–Pt(1)–Cl(2)	87.8(2)
C(2)–Pt(1)–Cl(2)	95.5(1)
P(1)–Pt(1)–Cl(2)	172.1(4)
Cl(1)–Pt(1)–Cl(2)	88.27(4)
C(1)–C(2)–Pt(1)	68.9(3)
C(3B)–C(2)–Pt(1)	118.6(5)
C(3A)–C(2)–Pt(1)	111.3(6)

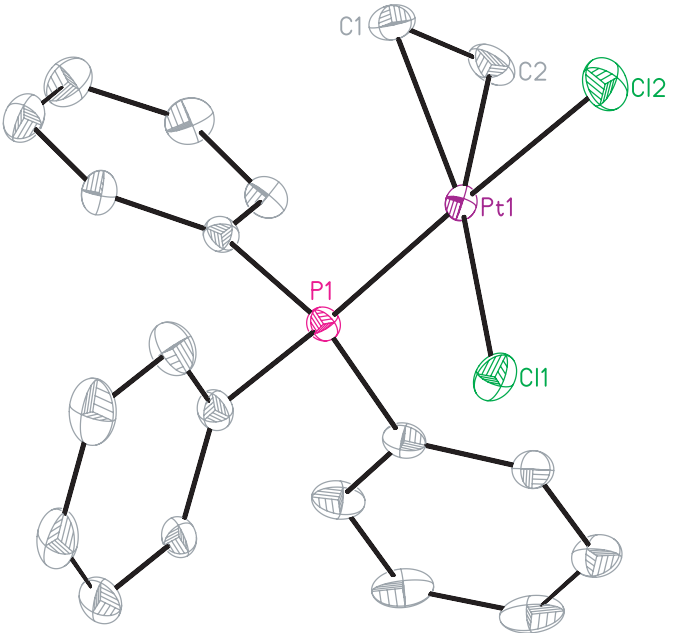

Figure 1. ORTEP diagram of *cis*-$PtCl_2(C_2H_4)(PPh_3)$ (50% thermal ellipsoids).

Pyramidalization represents the movement from sp^2 hybridization (planar) to sp^3 hybridization (tetrahedral). In the case of an alkene coordinated to platinum, movement of the π-electrons to the internal carbon would cause pyramidalization; simultaneously weakening the C–C bond while significantly increasing the Pt–C internal bond distance. Such a tautomer would also inhibit nucleophilic attack at the internal carbon, consistent with the results for NEt_2H attack which occurs terminal.

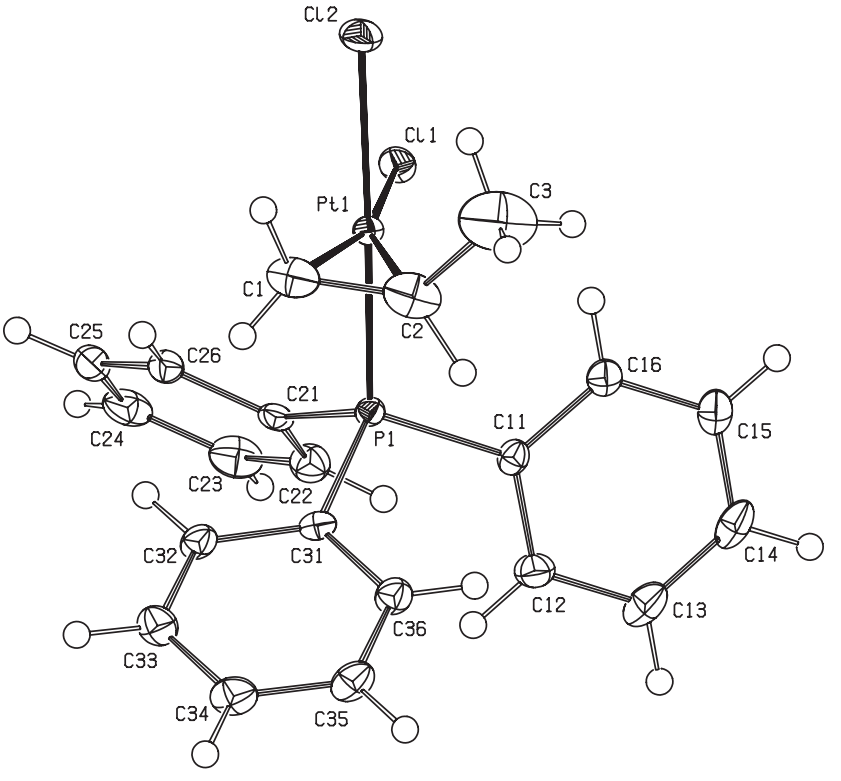

Figure 2. ORTEP diagram of *cis*-$PtCl_2(C_3H_6)(PPh_3)$, **4**.

***trans* Influence.** Table 5 shows comparative bond distances for all six compounds of generalized structure,

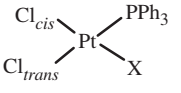

X = C_2H_4, C_3H_6, C_6H_{12}, CH_3CN, Cl(bridge)

Compounds **6** and **7** have different structures and will not be directly compared. In each case the Pt–Cl_{trans} bond length is longer than Pt–Cl_{cis} indicating that PPh_3 has the largest *trans* influence. The order of *trans* influence, as measured by Pt–Cl bond lengthening is [17]

$$PPh_3 > \text{hexene} \sim \text{1-propene} > \text{ethylene} > Cl^-(\text{bridge}) > CH_3CN$$

Measured on directly related complexes this provides a useful measure of relative *trans* influence.

Structures of 1, 2 and 6. Bond distances and angles for compounds **1**, **2** and **6** are shown in tables 6–8, respectively, and the atom numbering is shown in figures 4–6. Compounds **1** and **2** are square-planar complexes that could represent precursors to

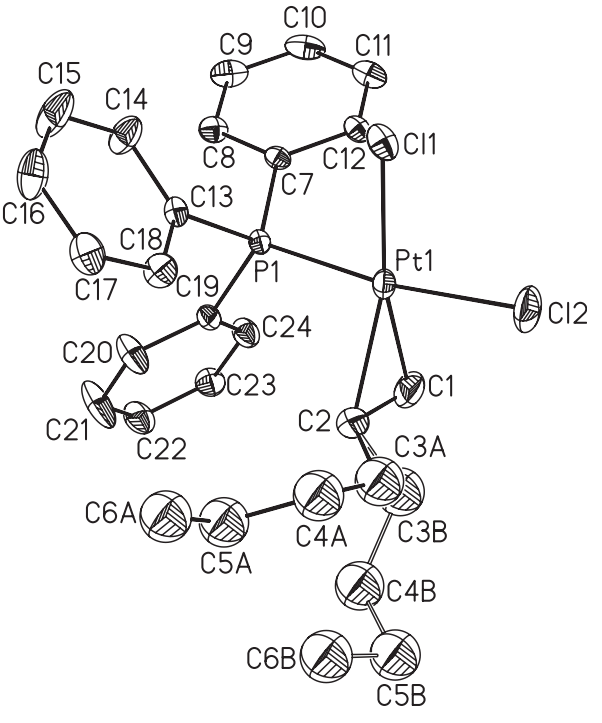

Figure 3. ORTEP diagram of *cis*-$PtCl_2(C_6H_{12})(PPh_3)$ (50% thermal ellipsoids).

Table 5. Comparative bond distances (Å).

Compound	Pt–P	Pt–Cl (*cis*)	Pt–Cl (*trans*)	Pt–X
1	2.211	2.278	2.410*	2.318
2	2.2516	2.2667	2.3637	1.978
3	2.2536	2.2964	2.436	2.147, 2.147
4	2.2610	2.3195	2.3623	2.146, 2.188
5	2.2517	2.3149	2.3514	2.144, 2.204
6**	2.2158	2.4110	–	–

* Bridging.
** Not Same Geometry.

Table 6. Bond lengths (Å) and angles (°) for $[PtCl_2PPh_3]_2XC_2H_2Cl_4$, **1**.

Pt(1)–P(1)	2.2114(17)
Pt(1)–Cl(1)	2.2779(16)
Pt(1)–Cl(2)	2.3178(17)
Pt(1)–Cl(2)#1	2.4096(17)
Cl(2)–Pt(1)#1	2.4096(17)
P(1)–Pt(1)–Cl(1)	89.69(6)
P(1)–Pt(1)–Cl(2)	95.64(6)
Cl(1)–Pt(1)–Cl(2)	174.49(6)
P(1)–Pt(1)–Cl(2)#1	178.94(6)
Cl(1)–Pt(1)–Cl(2)#1	90.78(6)
Cl(2)–Pt(1)–Cl(2)#1	83.88(6)
Pt(1)–Cl(2)–Pt(1)#1	96.12(6)

Symmetry transformations used to generate equivalent atoms: #1 $-x+1, -y+2, -z$.

Table 7. Bond lengths (Å) and angles (°) for $PtCl_2(CH_3CN)PPh_3$, **2**.

Pt(1)–N(1)	1.978(2)
Pt(1)–P(1)	2.2516(6)
Pt(1)–Cl(1)	2.2667(6)
Pt(1)–Cl(2)	2.3637(5)
N(1)–Pt(1)–P(1)	94.28(6)
N(1)–Pt(1)–Cl(1)	175.64(6)
P(1)–Pt(1)–Cl(1)	89.11(2)
N(1)–Pt(1)–Cl(2)	87.12(6)
P(1)–Pt(1)–Cl(2)	175.59(2)
Cl(1)–Pt(1)–Cl(2)	89.70(2)
C(1)–N(1)–Pt(1)	174.6(2)
N(1)–C(1)–C(2)	177.9(3)

Table 8. Bond lengths (Å) and angles (°) for $(PPh_3)ClPt(\mu\text{-}NEt_2CH_2CHCHCH_2NEt_2)PtCl(PPh_3)$, **6**.

Pt(1)–C(2B)	2.080(5)
Pt(1)–C(2A)	2.100(6)
Pt(1)–N(1)	2.157(3)
Pt(1)–P(1)	2.2158(9)
Pt(1)–Cl(1)	2.4110(7)
N(1)–C(1)	1.512(5)
C(1)–C(2A)#1	1.442(8)
C(1)–C(2B)#1	1.474(7)
C(2A)–C(1)#1	1.442(7)
C(2A)–C(2A)#1	1.53(2)
C(2B)–C(1)#1	1.474(7)
C(2B)–C(2B)#1	1.54(1)
C(2B)–Pt(1)–N(1)	82.5(2)
C(2A)–Pt(1)–N(1)	82.2(2)
C(2B)–Pt(1)–P(1)	95.1(2)
C(2A)–Pt(1)–P(1)	96.0(2)
N(1)–Pt(1)–P(1)	177.08(8)
C(2B)–Pt(1)–Cl(1)	168.6(2)
C(2A)–Pt(1)–Cl(1)	166.0(2)
N(1)–Pt(1)–Cl(1)	88.66(8)
P(1)–Pt(1)–Cl(1)	93.56(3)
C(1)–N(1)–Pt(1)	109.2(2)
C(2A)#1–C(1)–N(1)	114.0(4)
C(2B)#1–C(1)–N(1)	112.8(4)
C(1)#1–C(2A)–C(2A)#1	113.5(6)
C(1)#1–C(2A)–Pt(1)	122.2(4)
C(2A)#1–C(2A)–Pt(1)	105.5(6)
C(1)#1–C(2B)–C(2B)#1	110.0(6)
C(1)#1–C(2B)–Pt(1)	121.6(4)

Symmetry transformations used to generate equivalent atoms: #1 $-x+4$, $-y+4$, $-z-1$.

platinum alkene complexes. However, dissolution of *cis*-$PtCl_2$(alkene)(PPh_3) into CH_3CN shows gas evolution and formation of *cis*-$PtCl_2(CH_3CN)(PPh_3)$. The dimer, $Pt_2Cl_4(PPh_3)_2$ is useful for synthesis of *cis*-$PtCl_2(C_2H_4)(PPh_3)$.

Reaction of **3** with 1,3-butadiene gives a product characterized by NMR. Reaction of the butadiene complex with $NHEt_2$ gives a double anti-Markovnikov amination resulting in complex **6**. The structure of **6** is quite similar to the PEt_3 analogue reported a number of years ago [18]. The crucial feature of the structure of **6** is the doubly,

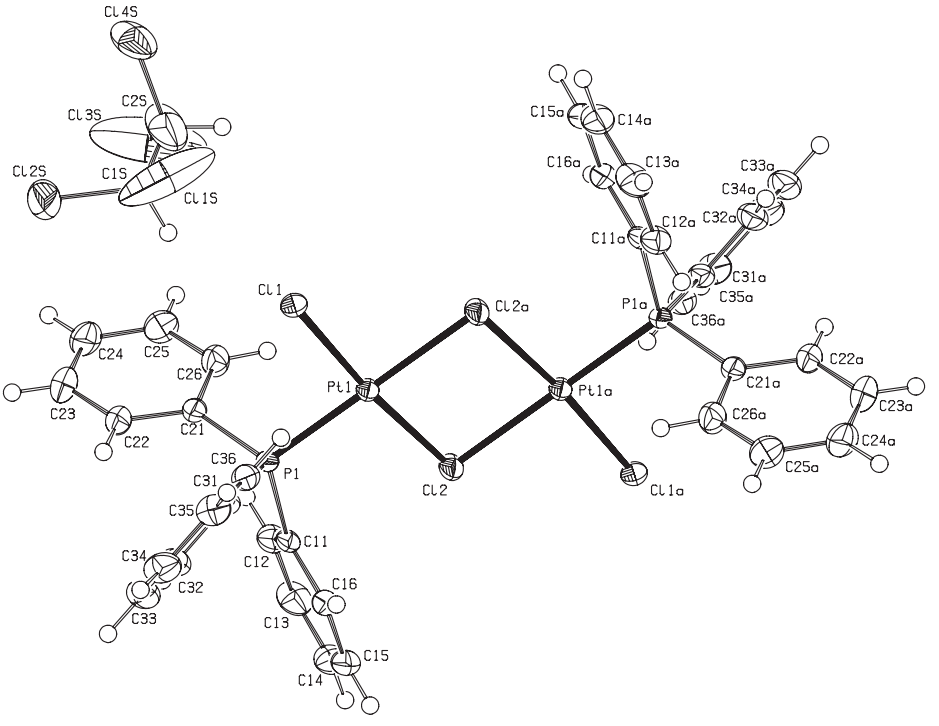

Figure 4. ORTEP diagram of $[PtCl_2(PPh_3)]_2X2C_2H_2Cl_4$, **1** (50% thermal ellipsoids).

anti-Markovnikov, aminated butadiene that is bidentate to two platinum centers through amine coordination and a carbon (alkyl) bond. The result is a dimeric unit with an η^4-$C_4H_6(NEt_2)_2$ bridging ligand. The platinum centers are distorted square planar with angles ranging from 82 to 96° (table 8). The Pt–PPh_3 and Pt–Cl distances are normal and indicate, as expected, a strong *trans* influence by the alkyl creating a longer Pt–Cl bond and a weak *trans* influence by the amine giving a shorter Pt–PPh_3 bond. The chelating, bridging ligand is composed of two five-member platinocycles with angles at platinum of ~82°.

Compound 7, $PtCl_2(\eta^4$-$C_4Me_4)(PPh_3)$. Reaction of 2-butyne with *cis*-$PtCl_2(C_2H_4)(PPh_3)$ results in a mixture of *cis*-$PtCl_2$(2-butyne)(PPh_3) and $PtCl_2(\eta^4$-$C_4Me_4)(PPh_3)$ as shown by NMR spectroscopies. The relatively broad resonance at $\delta = 1.59$ ppm in the ^{1}H NMR, shown in figure 7, is typical for coordinated 2-butyne, upfield of the free 2-butyne. The ^{1}H NMR resonance of the coordinated 1,2,3,4-cyclobutadiene at 1.39 shows both ^{195}Pt and ^{31}P coupling. To ascertain that the doublet arises from $J_{31_{P-Me}}$, phosphorus decoupling (figure S15) showed the resonance to collapse to a singlet. We could find no example where such coupling had previously been reported. The closest analogue, $PdCl_2(\eta^4$-$C_4(t\text{-}Bu)_2Me_2)(PPh_3)$ reports the Me resonance as a broad singlet at $\delta = 1.76$ ppm [19]. A platinum example, $Pt(CF_3)(\eta^4$-$C_4Me_4)(PMe_2Ph)_2^+$, reported 1.52 ppm with $J_{Pt-H} = 12.7$ Hz, but J_{P-H} was not resolved [20].

Recrystallization of the mixture resulted in single crystals of $PtCl_2(\eta^4$-$C_4Me_4)(PPh_3)$. The ORTEP plot with atom numbering is shown in figure 8 and selected bond distances

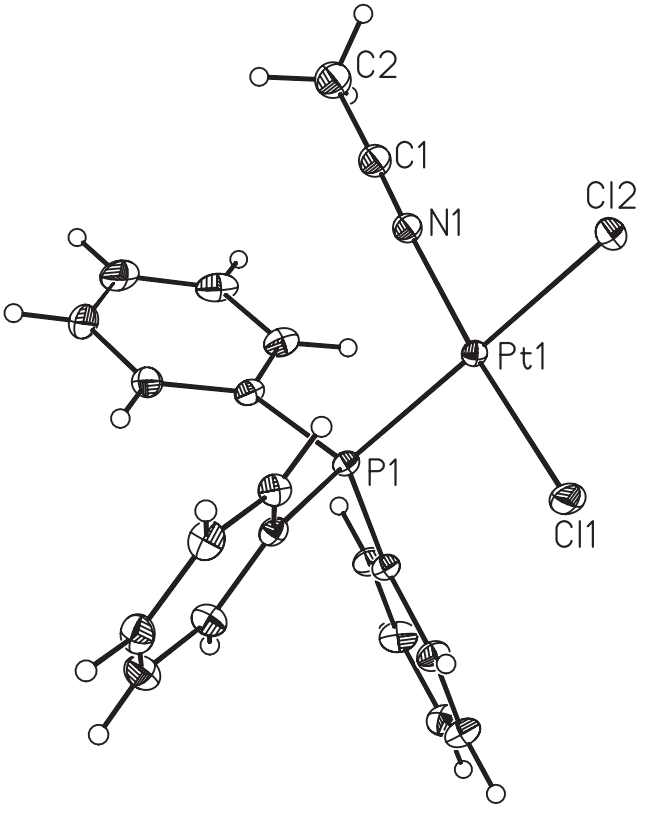

Figure 5. ORTEP diagram of *cis*-$PtCl_2(CH_3CN)(PPh_3)$.

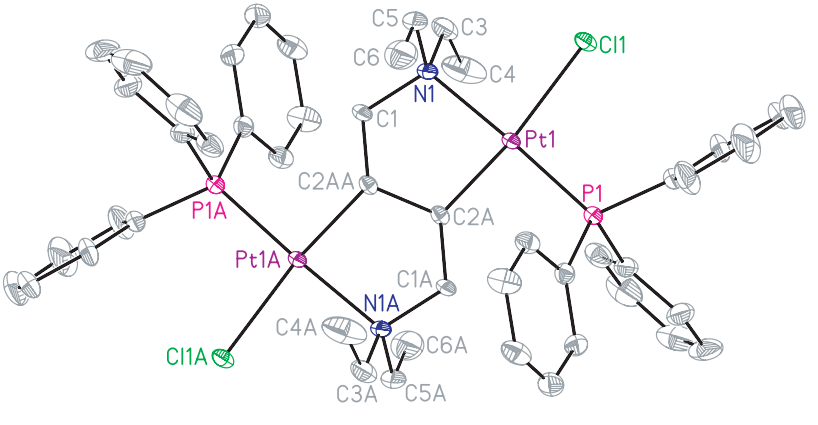

Figure 6. ORTEP diagram of $Pt_2Cl_2(C_4H_6(NEt_3)_2)_2(PPh_3)_2$ (50% thermal ellipsoids).

and angles are given in table 9. The geometry around Pt is best described as a "piano stool" with the legs being the PPh_3 and two chlorides. The angles around the cyclobutadiene sum to 360° indicating the planarity of the unit. Carbon–carbon bonds of cyclobutadiene complexes are typically in the range 1.44–1.50 Å [21];

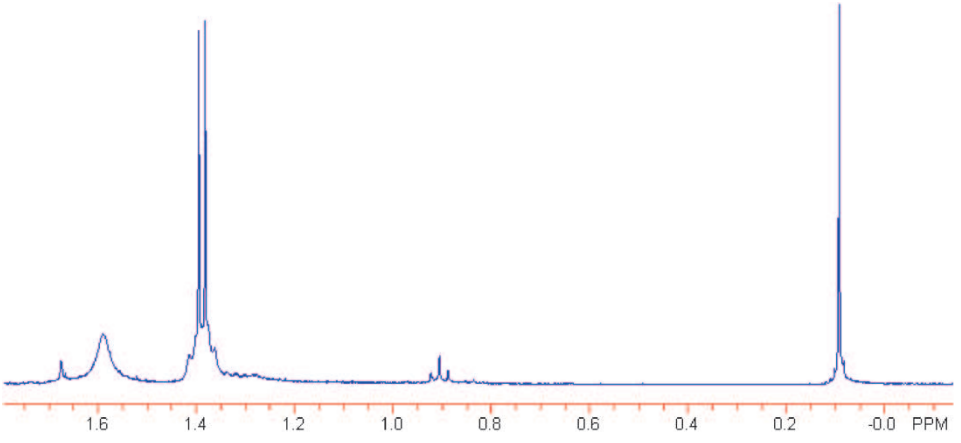

Figure 7. Partial ^{1}H NMR spectrum of a mixture of *cis*-$PtCl_2(C_4H_6)(PPh_3)$ and *cis*-$PtCl_2(\eta^4\text{-}C_4Me_4)(PPh_3)$.

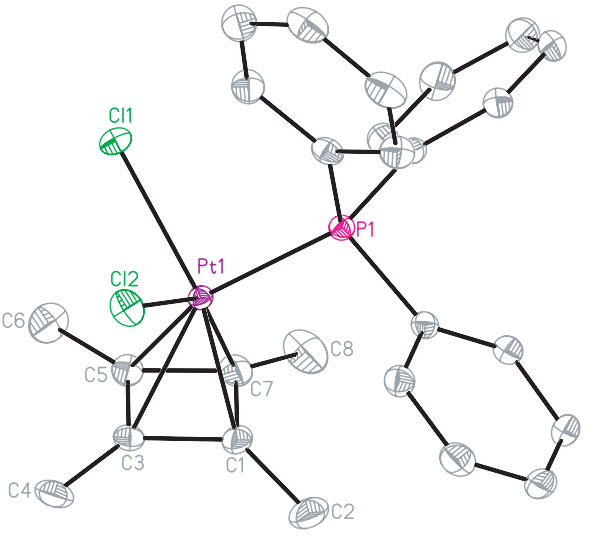

Figure 8. ORTEP diagram of *cis*-$PtCl_2(\eta^4\text{-}C_4Me_4)(PPh_3)$ (50% thermal ellipsoids).

the distances in $Pt(CF_3)(\eta^4\text{-}C_4Me_4)(PMe_2Ph)_2$ were 1.46–1.48 Å [22]. In **7** there is a marked asymmetry in the C–C bonds, C_1–C_7 (1.471(3) Å), C_1–C_3 (1.475(3) Å) and C_5–C_7 (1.473(3) Å) were equivalent and within the range previously observed. However, C_3–C_5 at 1.415(3) is out of the range previously observed and significantly shorter than the other three C–C bond distances. Previously observed asymmetry is usually manifested in lengthening of two bonds (rectangular) [23]. The Pt–C bond distances are more similar, Pt–C_1 (2.103(2) Å), Pt–C_7 (2.108(2) Å), Pt–C_5 (2.228(2) Å) and Pt–C_3 (2.237(2) Å) than the previous η^4-C_4Me_4 platinum complex (range 2.114–2.335 Å) [22] and indicate a slight tipping of the cyclobutadiene toward the platinum opposite to the shortest C–C bond (C_3–C_5).

Table 9. Bond lengths (Å) and angles (°) for **7**.

Pt(1)–C(1)	2.103(2)
Pt(1)–C(7)	2.108(2)
Pt(1)–C(5)	2.228(2)
Pt(1)–C(3)	2.237(2)
Pt(1)–P(1)	2.3163(5)
Pt(1)–Cl(2)	2.4407(4)
Pt(1)–Cl(1)	2.4675(4)
C(1)–C(7)	1.471(3)
C(1)–C(3)	1.475(3)
C(1)–C(2)	1.488(3)
C(3)–C(5)	1.415(3)
C(3)–C(4)	1.478(3)
C(5)–C(7)	1.473(3)
C(5)–C(6)	1.482(3)
C(7)–C(8)	1.481(3)
C(1)–Pt(1)–C(7)	40.91(8)
C(1)–Pt(1)–C(5)	56.78(7)
C(7)–Pt(1)–C(5)	39.61(7)
C(1)–Pt(1)–C(3)	39.58(7)
C(7)–Pt(1)–C(3)	56.61(8)
C(5)–Pt(1)–C(3)	36.96(7)
C(1)–Pt(1)–P(1)	107.59(5)
C(7)–Pt(1)–P(1)	109.35(5)
C(5)–Pt(1)–P(1)	148.04(5)
C(3)–Pt(1)–P(1)	145.33(5)
C(1)–Pt(1)–Cl(2)	109.45(6)
C(7)–Pt(1)–Cl(2)	147.42(6)
C(5)–Pt(1)–Cl(2)	120.01(5)
C(3)–Pt(1)–Cl(2)	92.23(5)
P(1)–Pt(1)–Cl(2)	90.82(2)
C(1)–Pt(1)–Cl(1)	147.26(6)
C(7)–Pt(1)–Cl(1)	110.25(6)
C(5)–Pt(1)–Cl(1)	91.28(5)
C(3)–Pt(1)–Cl(1)	118.19(5)
P(1)–Pt(1)–Cl(1)	96.20(2)
Cl(2)–Pt(1)–Cl(1)	91.96(2)
C(7)–C(1)–C(3)	88.9(2)
C(7)–C(1)–Pt(1)	69.7(1)
C(3)–C(1)–Pt(1)	75.1(1)
C(5)–C(3)–C(1)	91.0(2)
C(5)–C(3)–Pt(1)	71.2(1)
C(3)–C(5)–C(7)	91.2(2)
C(3)–C(5)–Pt(1)	71.9(1)
C(7)–C(5)–Pt(1)	65.8(1)
C(1)–C(7)–C(5)	88.9(2)
C(1)–C(7)–Pt(1)	69.4(1)
C(5)–C(7)–Pt(1)	74.6(1)

Cyclobutadiene complexes of transition metals have intrigued synthetic and theoretical chemists [24]. Our synthesis, from a metal with an open coordination site and an alkyne is well precedented and the mechanism has been described [21]. The Pt–C asymmetry seen in **7** was also observed in a platinum analogue, and attributed to crystal packing [22]. Crystal packing may also be involved in the unusual C–C bond variation for **7**. The coupling of both Pt to the Me 21.73 Hz (compared to 12.7 Hz for $Pt(CF_3)(\eta^4\text{-}C_4Me_4)(PMe_2Ph)_2$) and observation of the $^4J_{P-Me}$ indicate strong coupling within **7**. Certainly the NMR results provide no

indication of the asymmetry seen in the structure, consistent with crystal packing being responsible.

4. Conclusion

In this article we have reported the syntheses, characterization and crystal structure determinations of seven new complexes of platinum. All of these complexes are related to our examination of alkene complexes of platinum. Of special significance are: (1) the comparisons of the structures of the ethylene, propene and 1-hexene complexes, (2) the double anti-Markovnikov amination of 1,3-butadiene and (3) the cyclobutadiene complex formed from 2-butyne in the presence of *cis*-$PtCl_2(C_2H_4)(PPh_3)$.

Acknowledgement

The authors acknowledge the contribution of Robert Bogadi for the structure of **1**. R.S.P. is grateful for a Silbert Fellowship.

References

[1] W.C. Zeise. *Ann. Phys.*, **9**, 932 (1827).
[2] R. Pryadun, D. Sukumaran, R. Bogadi, J.D. Atwood. *J. Am. Chem. Soc.*, **126**, 12414 (2004).
[3] G.T. Kerr, A.E. Schweizer. *Inorg. Synth.*, **20**, 48 (1980).
[4] J.C. Bailar, H. Itatani. *Inorg. Chem.*, **4**, 1618 (1965).
[5] S.L. Hollis, S.J. Lippard. *J. Am. Chem. Soc.*, **105**, 3494 (1983).
[6] *Siemens: SMART and SAINT*. Data Collection and Processing Software for the SMART System, Siemens Analytical X-ray Instruments Inc., Madison, WI (1999).
[7] *SADABS: Area Detector Absorption Correction*, Siemens Industrial Automation, Inc., Madison, WI (1996).
[8] *SHELX97* [Includes SHELXS97, SHELXL97 and CIFTAB] Sheldrick, G. M. SHELX97, Programs for Crystal Structure Analysis (Release 97–2); Universität Göttingen: Göttingen, Germany (1997).
[9] SMART and SAINTPLUS, Area detector control and integration software. Ver. 6.01. Bruker Analytical X-ray Systems, Madison, Wisconsin, USA (1999).
[10] SHELXTL, An integrated system for solving, refining and displaying crystal structures from diffraction data, Ver. 5.10. Bruker Analytical X-ray Systems, Madison, Wisconsin, USA (1997).
[11] J. Chatt, N.P. Johnsen, B.L. Shaw. *J. Chem. Soc.*, 1662 (1963).
[12] M. Green, J.K.K Sarkan, I.M. Al-Najjar. *J. Chem. Soc.*, 1565 (1981).
[13] D.W. Price, M.G.B. Drew, K.K. Hii, J.M. Brown. *Chem. Eur. J.*, **6**, 4587 (2000) and references therein.
[14] H. B'gel, S. Tobisch, T. Nowak. *Int. J. Quantum Chem.*, **69**, 387 (1998).
[15] J. Uddin, S. Dapprich, G. Frenking, B.F. Yates. *Organometallics.*, **18**, 457 (1999).
[16] K. Morokuna, W.T. Borden. *J. Am. Chem. Soc.*, **113**, 1912 (1991).
[17] (a) J.D. Atwood. *Inorganic and Organometallic Reaction Mechanisms*, 2nd Edn, p. 49, VCH Publishers, Inc. (1997). (b)T.G. Appleton, H.C. Clark, L.E. Manzer, *Coord. Chem. Rev.*, **10**, 335 (1973).
[18] J.R. Briggs, C. Crocker, W.S. McDonald, B.L. Shaw. *J. Chem. Soc., Dalton*, 457 (1982).
[19] K. Mashima, D. Shimizu, T. Yamagatta, K. Tani. *Inorg. Chim. Acta*, **352**, 105 (2003).
[20] M.H. Chisholm, H.C. Clark. *J. Am. Chem. Soc.*, **94**, 1532 (1972).
[21] L.F. Veiros, G. Dazinger, K. Kirchner, M.J. Calhorda, R. Schmid. *Chem. Eur. J.*, **10**, 5860 (2004).
[22] D.B. Crump, N.C. Payne. *Inorg. Chem.*, **12**, 1663 (1973).
[23] (a) J.W. Chinn, M.B. Hall. *Inorg. Chem.*, **22**, 2759 (1982). (b) T.H. Lowry, S.K. Richardson. *Mechanism and Theory in Organic Chemistry*, 3rd Edn, p. 232, Harper & Row, New York (1987). (c) J.D. Fitzpatrick, L. Watts, G.F. Emerson, R. Pettit. *J. Am. Chem. Soc.*, **87**, 3254 (1965). (d) R. Pettit. *J. Organomet. Chem.*, **100**, 205 (1975).
[24] (a) Review of the Histroy – D. Seyferth. *Organometallics*, **22**, 2 (2003). (b) P.K. Baker, H. Silgram. *Trends in Organometallic Chemistry*, **3**, 21 (1999). (c) A. Efraty. *Chem. Rev.*, **77**, 691 (1977). (d) A. Sekiguchi, T. Matsuo, M. Tanaka. *Organometallics*, **21**, 1072 (2002). (e) S.-Y. Chu, R. Hoffmann. *J. Phys. Chem.*, **86**, 1289 (1982).